APPENDIX A

Table A1: WDS conditions used in this study for EMPA analysis.

Element	Fluorescence line analyzed		Standard	Counting time	Detection limit [ppm]
Fe	Kα	LIF	Hematite	16|8	215
Mn	Kα		Bustamite	30|15	100
Al	Kα	TAP	Sanidine	16|8	65
W	Lα		$CaWO_4$	30|15	240
As	Kα	LIF	GaAs	30|15	460
P	Kα		Apatite	16|8	110
Si	Kα	TAP	Diopside	16|8	100
Sb	Lα		Stibnite	30|15	430
Mo	Lα		Mo-metal	30|15	890
Ca	Kα		Diopside	16|8	65
Mg	Kα	TAP	Diopside	16|8	75

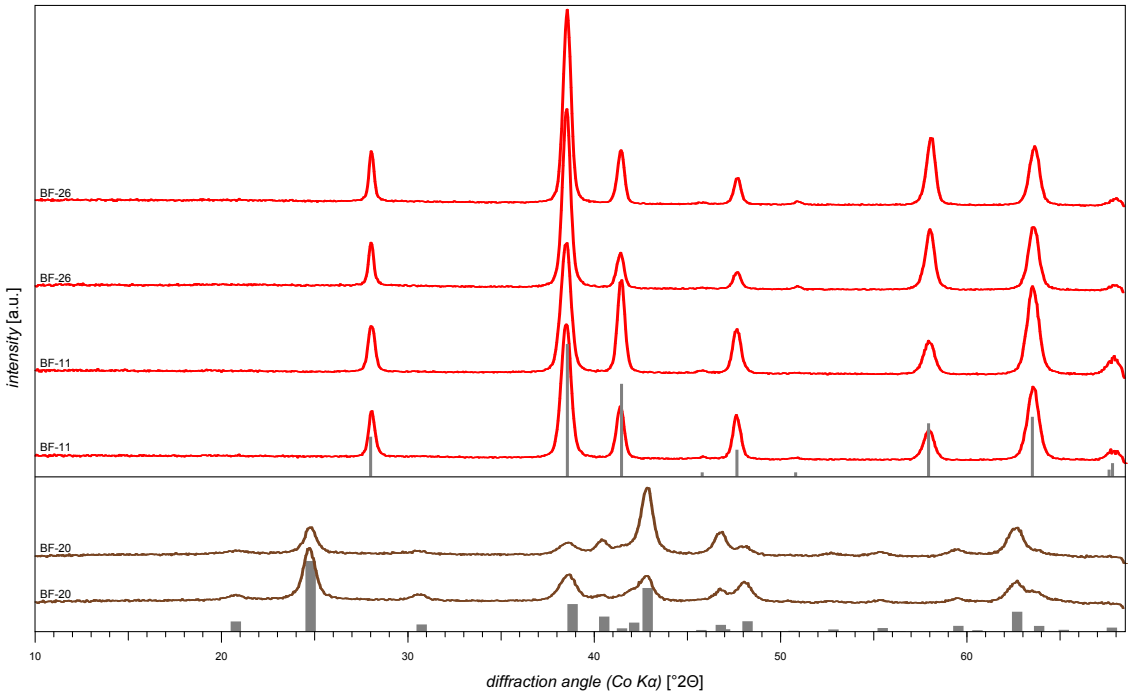

FIGURE A1: μXRD pattern of hematite (BF-11 and BF-26; upper part) and goethite (BF-20; lower part) from the Black Forest. The measuring spots were set to regions with the most elevated W concentration of the samples detected by EMPA (hematite: ~1.4 wt% WO_3; goethite: ~0.2 wt% WO_3).

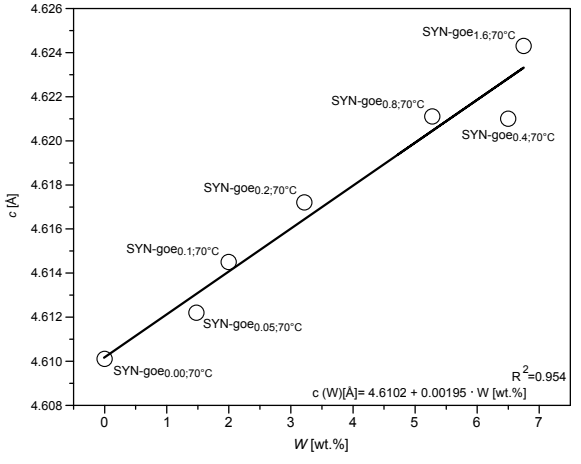

FIGURE A2: Crystallographic cell parameter c according to the W concentration of the syntetic powder samples (cf. Table 1).

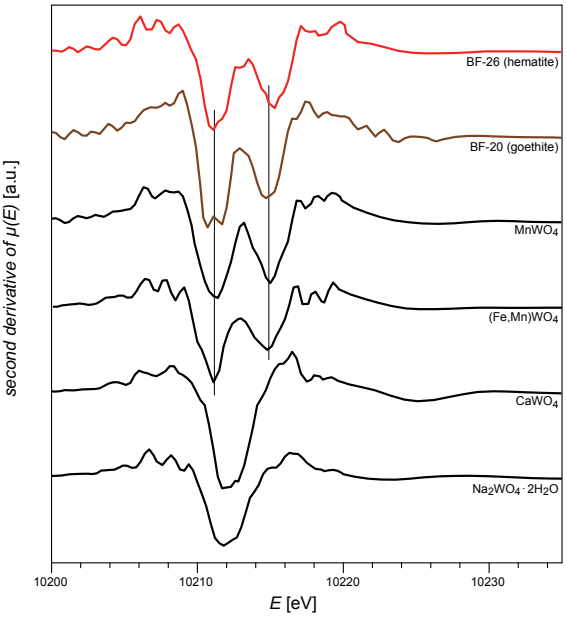

FIGURE A3: Second derivatives of W L3 XANES spectra of the reference substances Na2WO4·2H2O, CaWO4, wolframite ((Fe,Mn)WO4), hübnerite (MnWO4) and the samples hematite BF-26 and goethtie BF-20. Lines indicate the peak splitting for the reference substances with distorted octahedra and of two of the samples Splitting for heamtite BF-26 is slightly larger than for wolramtie, hübnerite and goethite BF-20.

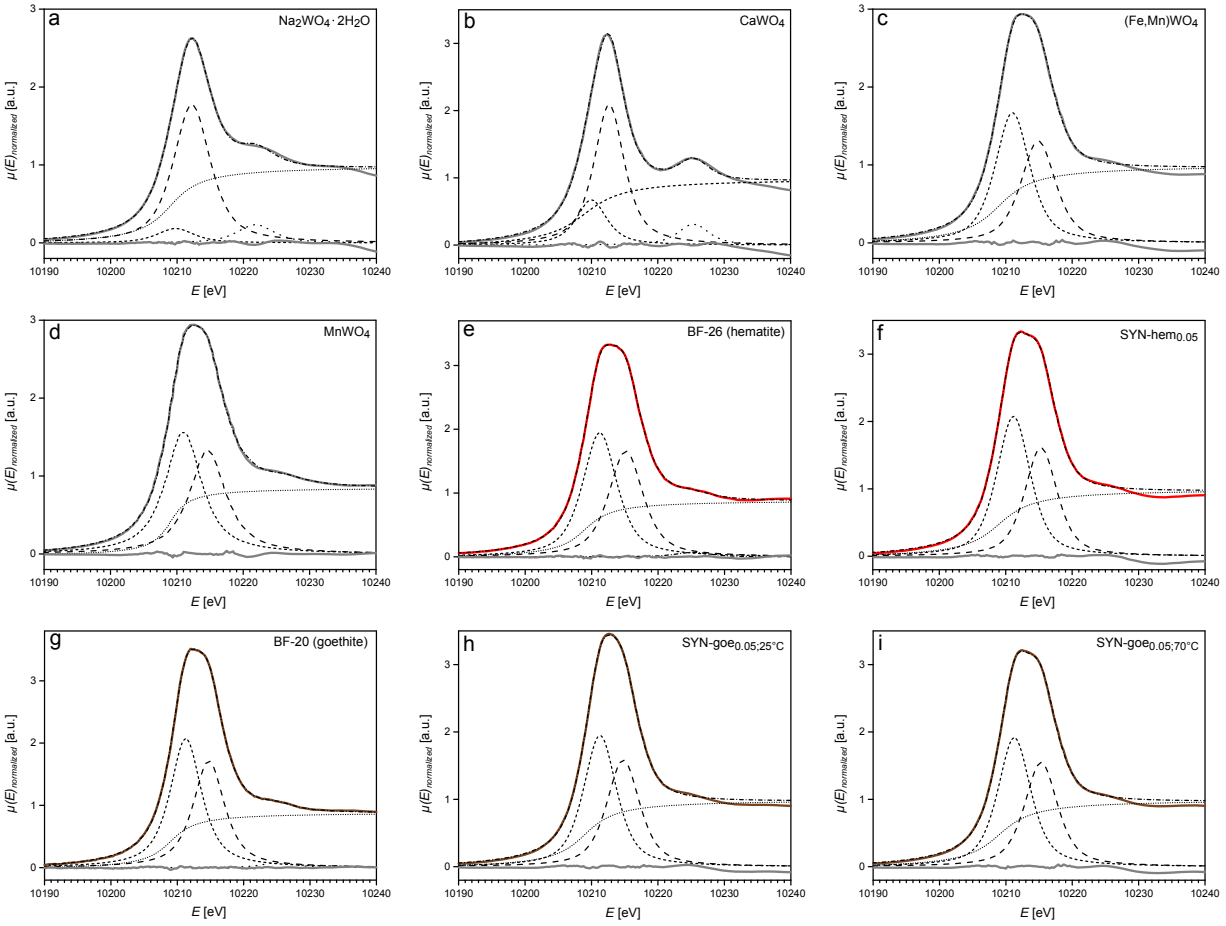

FIGURE A4.1: Deconvolution of W L_3 XANES spectra of reference substances: (a) $Na_2WO_4 \cdot 2H_2O$, (b) scheelite ($CaWO_4$), (c) wolframite ($(Fe,Mn)WO_4$), (d) hübnerite ($MnWO_4$), and samples: (e) hematite (BF-26) and (g) goethite (BF-20), (h) goethite SYN-$goe_{0.05;25°C}$, (i) goethite SYN-$goe_{0.05;70°C}$, and (f) hematite (SYN-$hem_{0.05}$). Measured data of the edge illustrated as solid lines, fitting peaks as dashed or dotted lines and the accumulation of the fits as dot-dash lines. Solid lines at the bottom represent the deviation between the fit accumulation and the measured data.

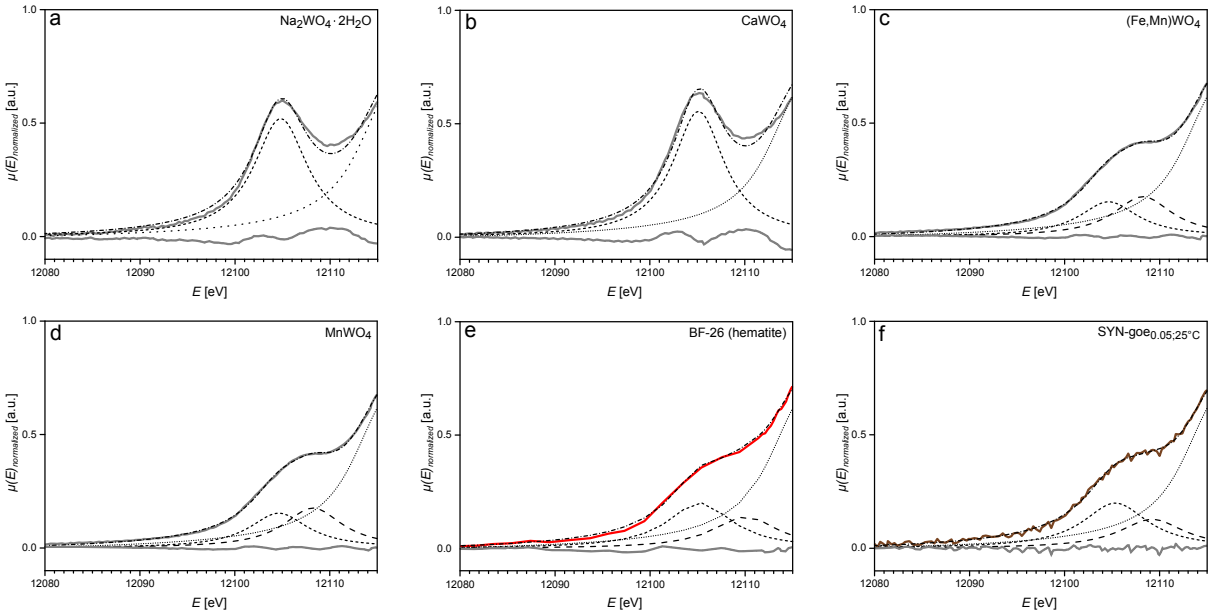

FIGURE A4.2: Deconvolution of W L_1 XANES spectra of reference substances: (a) $Na_2WO_4 \cdot 2H_2O$, (b) scheelite ($CaWO_4$), (c) wolframite ((Fe,Mn)WO_4), (d) hübnerite ($MnWO_4$), and samples: (e) hematite (BF-26) and (f) goethite SYN-$geo_{0.05;25°C}$. For (c) to (f) two peaks have been used to fit the pre-edge; their intensities have been summed up. Measured data of the edge illustrated as solid lines, fitting peaks as dashed or dotted lines and the accumulation of the fits as dot-dash lines. Solid lines at the bottom represent the deviation between the fit accumulation and the measured data.

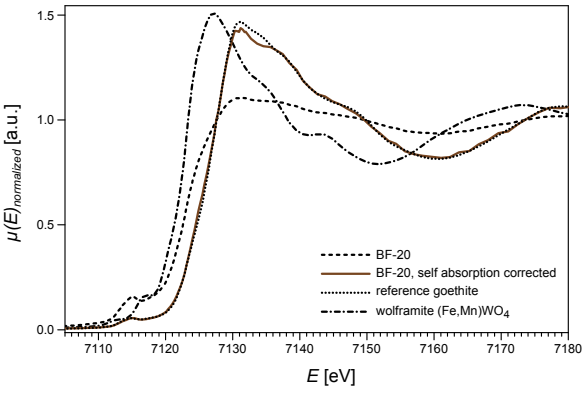

FIGURE A5.1: Fe K XANES spectra of natural goethite BF-20, after self absorption correction, compared to a reference goethite and wolframite.

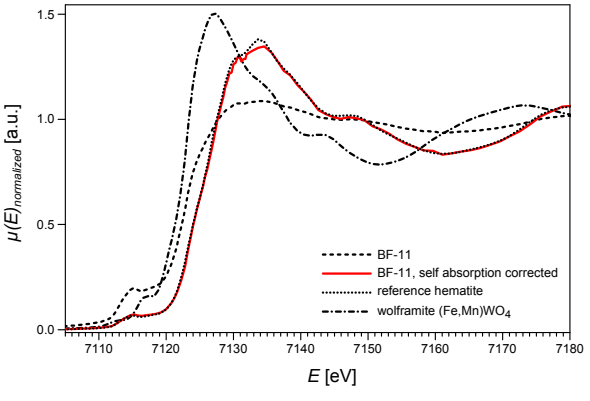

FIGURE A5.2: Fe K XANES spectra of natural hematite BF-11, after self absorption correction, compared to a reference hematite and wolframite.

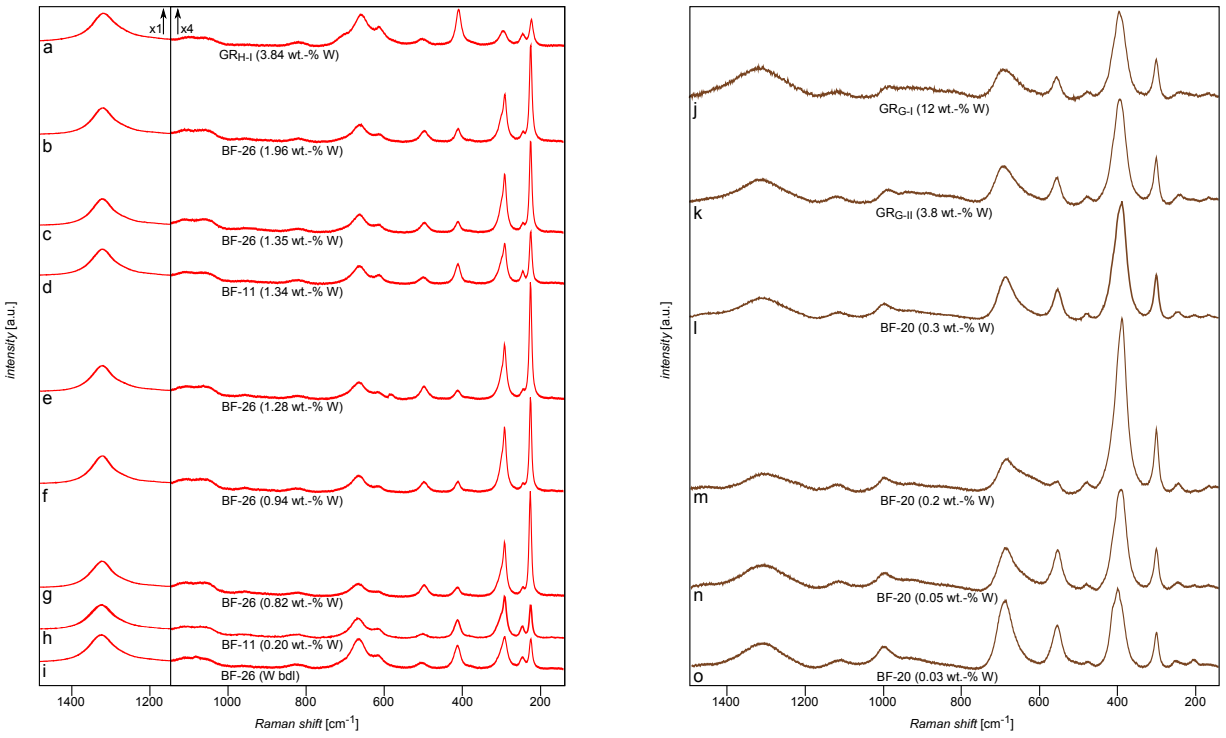

FIGURE A6: Raman spectra of natural samples with different W concentrations. Left side (a-i) hematite and right side (j-o) goethite. (a) GR_{H-I}, (d and h) BF-11, (b, c, e, f, g and i) BF-26; (j) GR_{G-I}, (k) GR_{G-II}, (l, m, n and o) BF-20. At each spectra, the W concentration is indicated and decreases from the top to bottom spectra. The subdivision of the left figure (hematite) indicates a 4-time raised intensity scale of the right part of each spectra.

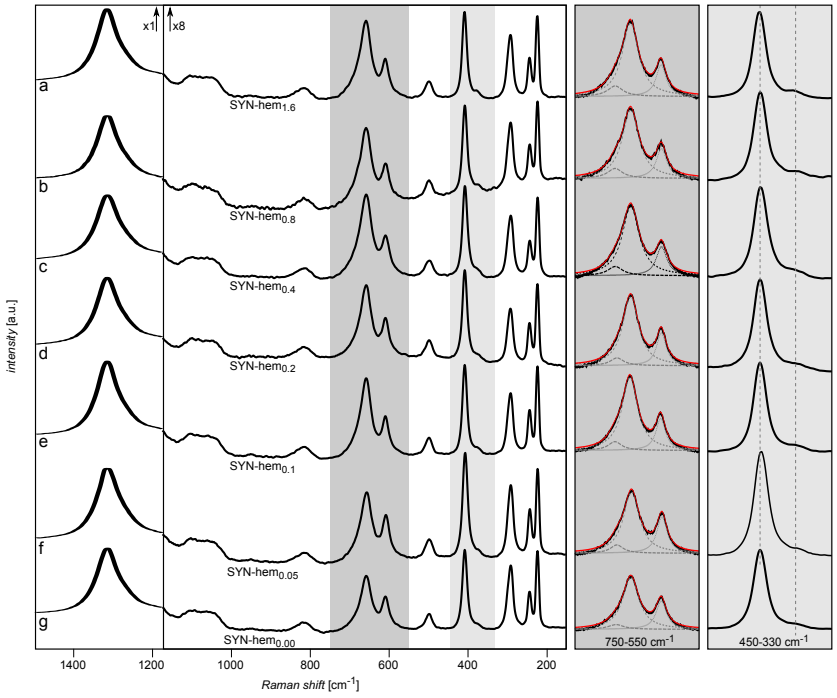

FIGURE A7: Raman spectra of synthetic hematite samples with decreasing W concentration from top to bottom: (a) SYN-hem$_{1.6}$, (b) SYN-hem$_{0.8}$, (c) SYN-hem$_{0.4}$, (d) SYN-hem$_{0.2}$, (e) SYN-hem$_{0.1}$, (f) SYN-hem$_{0.05}$ and (g) SYN-hem$_{0.00}$. The subdivision indicates an 8-time raised intensity scale of the right part of each spectra. The grey highlighted areas are in detail on the right side showing the 450-330 cm^{-1} and 750-550 cm^{-1} intercepts of the spectra. Peaks of the 750-550 cm^{-1} intercept spectra fits represent the dashed lines and their accumulation the dash-dot lines.

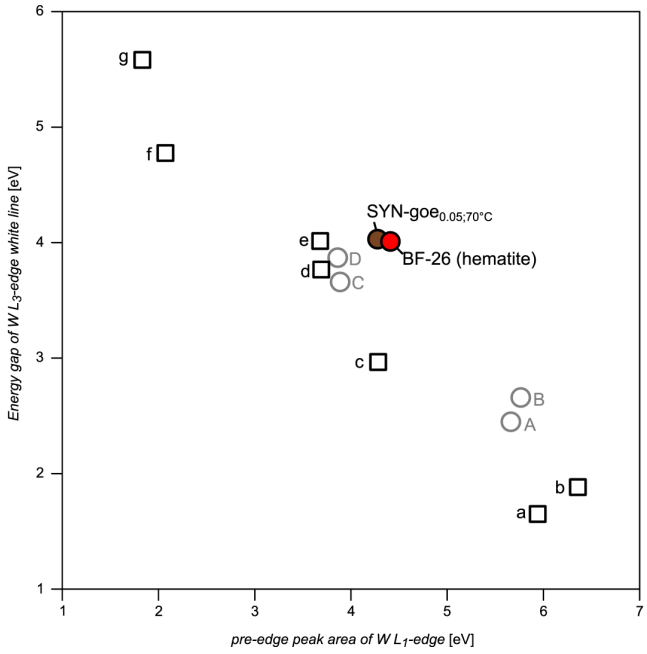

FIGURE A8: Pre-edge peak area of W L_1-edge XANES spectra in function of the energy gap of the split W L_3-edge white line of reference samples: This study $Na_2WO_4 \cdot 2H_2O$ (A), $CaWO_4$ (scheelite) (B), $MnWO_4$ (hübnerite) (C) and $(Fe,Mn)WO_4$ (wolframite) (D) (open circles) and of Yamazoe et al., 2008 (taken from their Figure 11): Na_2WO_4 (a), $Sc_2W_3O_{12}$ (b), $H_3PW_{12}O_{40}$ (c), WO_3 (d), $(NH_4)_{10}W_{12}O_{41} \cdot 5H_2O$ (e), Cr_2WO_6 (f) Ba_2NiWO_6 (g) (open squares). Values of the sample SYN-$goe_{0.05;70°C}$ and BF-26 plot close to hübnerite, wolframite and WO_3 data indicating similar W coordination and electronic structure of distorted WO_6 octahedra.